Monthly Notices
of the
ROYAL ASTRONOMICAL SOCIETY

MNRAS **472,** 4110–4116 (2017)
Advance Access publication 2017 September 6

doi:10.1093/mnras/stx2295

Asteroseismic masses of retired planet-hosting A-stars using SONG

Dennis Stello,[1,2,3]★ Daniel Huber,[4,2,5,3] Frank Grundahl,[3] James Lloyd,[6] Mike Ireland,[7] Luca Casagrande,[7] Mads Fredslund,[3] Timothy R. Bedding,[2,3] Pere L. Palle,[8] Victoria Antoci,[3] Hans Kjeldsen[3] and Jørgen Christensen-Dalsgaard[3]

[1]*School of Physics, University of New South Wales, NSW 2052, Australia*
[2]*Sydney Institute for Astronomy (SIfA), School of Physics, University of Sydney, NSW 2006, Australia*
[3]*Department of Physics and Astronomy, Stellar Astrophysics Centre, Aarhus University, DK-8000 Aarhus C, Denmark*
[4]*Institute for Astronomy, University of Hawaii, 2680 Woodlawn Drive, Honolulu, HI 96822, USA*
[5]*SETI Institute, 189 Bernardo Avenue, Mountain View, CA 94043, USA*
[6]*Department of Astronomy, Cornell University, Ithaca, NY 14850, USA*
[7]*Mount Stromlo Observatory, Research School of Astronomy & Astrophysics, The Australian National University, ACT 2611, Australia*
[8]*Instituto de Astrof sica de Canarias, E-38200 La Laguna, Tenerife, Spain*

Accepted 2017 August 31. Received 2017 August 31; in original form 2017 July 25

ABSTRACT

To better understand how planets form, it is important to study planet occurrence rates as a function of stellar mass. However, estimating masses of field stars is often difficult. Over the past decade, a controversy has arisen about the inferred occurrence rate of gas-giant planets around evolved intermediate-mass stars – the so-called 'retired A-stars'. The high masses of these red-giant planet hosts, derived using spectroscopic information and stellar evolution models, have been called into question. Here, we address the controversy by determining the masses of eight evolved planet-hosting stars using asteroseismology. We compare the masses with spectroscopic-based masses from the Exoplanet Orbit Database,which were previously adopted to infer properties of the exoplanets and their hosts. We find a significant one-sided offset between the two sets of masses for stars with spectroscopic masses above roughly 1.6 $M_{\odot}$, suggestive of an average 15–20 per cent overestimate of the adopted spectroscopic-based masses. The only star in our sample well below this mass limit is also the only one not showing this offset. Finally, we note that the scatter across literature values of spectroscopic-based masses often exceeds their formal uncertainties, making it comparable to the offset we report here.

Key words: techniques: radial velocities – stars: fundamental parameters – stars: interiors – stars: oscillations.

1 INTRODUCTION

One way to understand how planets form is to find relationships between the occurrence rates of exoplanets and the fundamental properties of their host stars, such as mass. The search for exoplanets has mainly been focused on cool main-sequence stars below $\sim$1.4 $M_{\odot}$ because their planets are easier to detect (Johnson et al. 2006). To extend the mass range of exoplanet host targets, Johnson et al. (2006) searched for planets around cool evolved intermediate-mass stars, dubbed retired A-stars[1], which were once hotter main-sequence stars, from which planet occurrence rates could be inferred. To estimate stellar mass, they used an isochrone grid-modelling approach based on spectroscopic input observables (log$g$, $T_{\rm eff}$ and [Fe/H]). From this, Johnson et al. (2007a,b) reported general increased planet occurrence rates but a paucity of planets in short-period orbits.

However, the mass estimates of the retired A-stars were subsequently called into question by Lloyd (2011), who argued it was statistically unlikely that the sample, which he extracted from the Exoplanet Orbit Database (EOD; Wright et al. 2011), would include so many relatively massive stars, given their location in the HR-diagram. This led to further investigations by Johnson, Morton & Wright (2013), Lloyd (2013) and Schlaufman & Winn (2013), but without a clear resolution.

Sparked by the new space-based era of high-precision time series photometry, a recent surge of results from the asteroseismology of red giants has shown that detailed and highly precise information

★ E-mail: d.stello@unsw.edu.au

[1] While not all the retired A-stars are strictly speaking old A-stars (some are less massive), we adopt this previously dubbed 'group-name' for simplicity.

© 2017 The Authors
Published by Oxford University Press on behalf of the Royal Astronomical Society

Downloaded from https://academic.oup.com/mnras/article/472/4/4110/4107124 by guest on 23 April 2024

can be obtained about these stars (e.g. Bedding et al. 2011; Beck et al. 2012; Mosser et al. 2012; Stello et al. 2016). In particular, stellar mass can be measured (Stello et al. 2008; Kallinger et al. 2010), which makes asteroseismology an obvious way to resolve the dispute about the retired A-star planet-host masses.

One retired A-star, the red-giant-branch star HD 185351, was observed by *Kepler*. The initial analysis by Johnson et al. (2014) found different masses spanning 1.60–1.99 $M_\odot$ depending on the combination of seismic and interferometric input, as compared to 1.87 $M_\odot$ for the purely spectroscopic-based mass. The seismic inputs were $\Delta\nu$, the frequency spacing between overtone modes, and ν_{max}, the frequency of maximum power. Recent results including also the period spacing between dipole mixed modes (ΔP) as an extra seismic quantity, and non-standard physics provided stronger constraints, indicating more definitively a lower mass of 1.58 ± 0.03 $M_\odot$ for this star (Hjørringgaard et al. 2017).

Even more recently, Campante et al. (2017) used K2 observations of another retired A-star, HD 212771, to measure its mass from asteroseismology to be 1.45 ± 0.10 $M_\odot$. Despite this star being in a very similar evolutionary stage to HD 185351, the seismic mass of HD 212771 was larger than the original spectroscopy-based value of 1.15 ± 0.08 $M_\odot$ (Johnson et al. 2010). However, subsequent spectroscopic investigations also estimated its mass to be larger (1.51 ± 0.08 $M_\odot$, Mortier et al. 2013; 1.60 ± 0.13 $M_\odot$, Jofré et al. 2015) than reported by Johnson et al. (2010).

With only two seismic targets showing inconclusive results, it is still not clear if the stellar masses are systematically overestimated in the planet discovery papers, which would affect conclusions about how planet occurrence rates depend on stellar mass, and potentially lead to a different explanation for the high occurrence of planets in the retired A-star sample (currently attributed to the high stellar mass).

In this paper, we investigate the retired A-star mass controversy by observing eight planet-hosting red giants using the ground-based SONG telescope to detect solar-like oscillations. This allows us to estimate the stellar mass using asteroseismology, and hence to investigate whether there is a general problem with the previously adopted mass scale of the retired A-star planet hosts.

2 TARGET SELECTION AND OBSERVATIONS

We note that the stars in question are often referred to as 'subgiants' following the historical spectroscopic classification that some of them carry. However physically, they are either helium-core burning (red-clump stars), or burning hydrogen in a shell around an inert helium core with luminosities below the red clump but already in the red-giant-branch phase (with radius, and hence luminosity increasing rapidly at roughly constant $T_{\rm eff}$). We therefore refer to them as red giants. The mass controversy is starkest for the red-giant-branch stars. Their evolutionary speed is highly mass-dependent, making it much more likely to find such stars with $M \lesssim 1.5\,M_\odot$ than $M \gtrsim 1.5\,M_\odot$, as illustrated by the mass-dependent density of dots along the stellar evolution tracks in Fig. 1. Genuine retired A-stars are expected to be rare.

We selected our targets from the EOD[2]. The initial criteria were $3.75 > \log(T_{\rm eff}/{\rm K}) > 3.65$ ($5623\,K > T_{\rm eff} > 4467\,K$) and $\log(L/L_\odot) > 0.75$ ($L > 5.62\,L_\odot$). For this, we used $T_{\rm eff}$ from the EOD and derived luminosity using the *Hipparcos* distance,

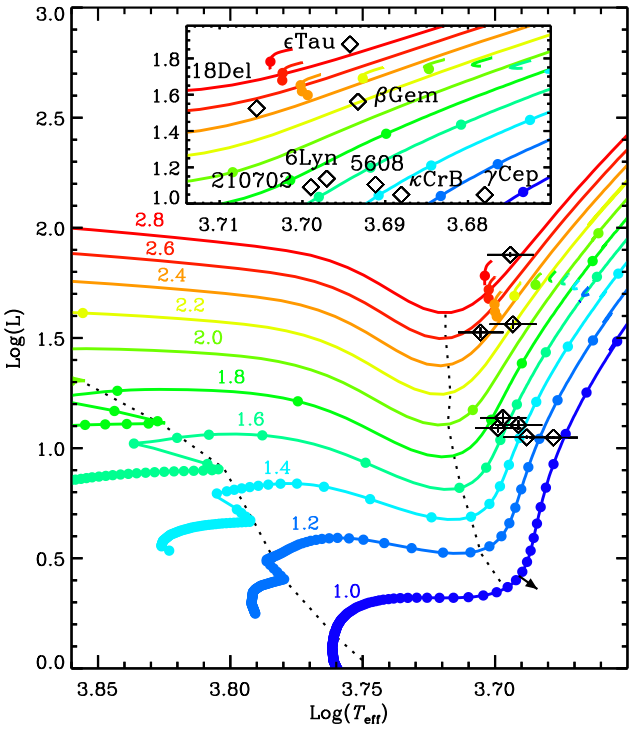

Figure 1. HR-diagram showing MESA (Paxton et al. 2013) stellar evolution tracks of solar metallicity from Stello et al. (2013). The likelihood of finding a star in a given state of evolution (for a given mass) is illustrated by the filled dots along each track, which are equally spaced by 50 Myr in stellar age. Masses in solar units are shown. The black arrow near the bottom of the 1.0 $M_\odot$ red-giant branch illustrates how much the tracks shift if [Fe/H] is increased by 0.2 dex. Dotted fiducial lines are indicative of the transitions from the main sequence to subgiants, and from the rapidly cooling subgiants (at roughly constant radius) to the rapidly expanding red giants (at roughly constant $T_{\rm eff}$). The planet-hosting targets are shown with diamonds and the adopted 1σ error bars. The helium-core burning models are those within the range $1.6 \lesssim \log(L) \lesssim 1.8$. The inset shows a close-up.

V magnitude and a metallicity-dependent bolometric correction (Alonso, Arribas & Martínez-Roger 1999, equation 18), ignoring extinction due the proximity of our targets. From this initial selection, we chose the six brightest stars in the northern sky with $\log g > 3$ and the two brightest stars with $\log g < 3$ (see Fig. 1).

The time-resolved radial velocities were obtained with the robotic 1-m Hertzsprung SONG telescope on Tenerife (Andersen et al. 2014; Grundahl et al. 2017) during the period from 2014 August to 2015 December using its échelle spectrograph. Our strategy was to observe the stars long enough that the frequency of maximum oscillation power, ν_{max}, could be determined from single-site observations to a precision of about 15 per cent. This should allow us to make conclusions about difference in mass between seismology- and spectroscopy-based values in an ensemble sense even if not on a single star basis. To determine the length of time series observations required, we used data of the red-giant ξ Hya obtained using the Coralie spectrograph on the 1.2-m Euler telescope at La Silla (Frandsen et al. 2002), which has similar performance to SONG. These data comprised 30 full consecutive nights of observations that clearly showed stellar oscillations with frequencies centred at ν_{max} ~90 μHz (Stello et al. 2004). By splitting the series into multiple segments, we found that the intrinsic ν_{max} scatter across segments

[2] www.exoplanets.org

Downloaded from https://academic.oup.com/mnras/article/472/4/4110/4107124 by guest on 23 April 2024

Table 1. Observing parameters for the targets.

Star	V	$T_{\rm exp}$ (s)	$N_{\rm exp}$	R	$N_{\rm night}^{\rm obs}$	$N_{\rm night}^{\rm span}$	$\sigma_{\rm RV}$ ($\rm m\,s^{-1}$)
ϵ Tau*	3.53	180	941	77k	8	9	2.76
β Gem*	1.15	20	5410	77k	5	6	1.61
18 Del*	5.51	600	358	77k	9	11	2.53
γ Cep	3.21	120	1758	90k	13	13	2.00
HD 5608	6.00	600	171	77k	7	9	2.70
κ CrB	4.79	300	495	90k	7	13	2.11
6 Lyn	5.86	600	206	77k	5	5	3.12
HD 210702	5.93	600	126	77k	5	7	2.52

V: magnitude.
$T_{\rm exp}$: exposure time.
$N_{\rm exp}$: number of exposures.
R: spectrograph resolution.
$N_{\rm night}^{\rm obs}$: number of observing nights.
$N_{\rm night}^{\rm span}$: length of time series.
$\sigma_{\rm RV}$: mean radial-velocity precision.
*Most likely red-clump stars (see Fig. 1); not in conflict with the known planet orbits.

reached about 15 per cent if the segments were 5–10 d long;[3] this guided the required minimum observation length per star.

The lengths of the observations varied between 5 and 13 nights, and the number of spectra for each target varied from night to night due to constraints from weather, visibility and the execution of other observing programmes, which was not critical for our purpose of measuring $\nu_{\rm max}$ to within 15 per cent. However, we do note that such short single-site data on red giants do not allow us to measure $\Delta\nu$ or individual mode frequencies. The SONG échelle spectroscopy made use of an iodine cell for high-precision wavelength calibration. Exposure times were tuned to ensure sufficiently sampling of the oscillations while keeping the spectral signal-to-noise ratio above ∼100 in the wavelength range with a large number of iodine lines. Table 1 lists the basic parameters for the data obtained for each target.

The data reduction into 1D spectra was performed using an extraction pipeline based on the C++ implementation by Ritter, Hyde & Parker (2014) of the IDL routines by Piskunov & Valenti (2002) for order tracing and extraction of échelle spectra. The calculation of the radial-velocity time series was performed using the ISONG software (Antoci et al. 2013; Grundahl et al. 2017), which follows the approach by Butler et al. (1996). We applied a post-processing high-pass filter with a characteristic cut-off frequency of ∼3 μHz to remove any slow trends in the data, which could otherwise result in power leaking into the frequency range of the stellar oscillations. The final time series are shown in Fig. 2. The radial-velocity scatter, which typically ranges about $\pm 10\,\rm m\,s^{-1}$, is dominated by the oscillations, as illustrated by the insets for the stars β Gem and 6 Lyn.

3 STELLAR PARAMETERS

To make predictions of the expected seismic signal, $\nu_{\rm max}$, we used the empirical scaling relation by Brown et al. (1991) and Kjeldsen & Bedding (1995), which relies on the assumption that $\nu_{\rm max}$ is proportional to the acoustic cut-off frequency, hence

$$\nu_{\rm max}/\nu_{\rm max,\odot} \simeq \frac{M/{\rm M}_\odot}{(R/{\rm R}_\odot)^2(T_{\rm eff}/T_{\rm eff,\odot})^{0.5}} = \frac{M/{\rm M}_\odot (T_{\rm eff}/T_{\rm eff,\odot})^{3.5}}{L/{\rm L}_\odot}, \quad (1)$$

where $\nu_{\rm max,\odot} = 3090$ μHz (Huber et al. 2009) and $T_{\rm eff,\odot} = 5777$ K. This empirical relation has been verified to be good to within at least 5 per cent for red giants of near solar metallicity (Huber et al. 2012; Gaulme et al. 2016, see also Section 4.1). For each star, we therefore required estimates of mass, luminosity and effective temperature. We adopted the spectroscopic-based masses from the EOD (Table 2, column 6), which are ultimately those we want to compare with the seismology. We note that these masses have been updated compared to those disputed by Lloyd (2011, table 2, column 7), and we comment on those earlier mass results later.

To calculate luminosities, we used *Hipparcos* parallaxes (Table 2, column 5), spectroscopic $T_{\rm eff}$ and [Fe/H] from the EOD sourced from the same papers as the adopted mass to be self-consistent for the later comparison (Table 2, columns 3 and 4), and Tycho $V_{\rm T}$ photometry (Høg et al. 2000) as input to the direct method implemented in ISOCLASSIFY (Huber et al. 2017)[4]. In summary, we sampled distances following a posterior calculated from the *Hipparcos* parallax. The precise parallaxes make the posteriors insensitive to the adopted prior. For each distance sample, we calculated the extinction, $A_{\rm V}$, using the map by Green et al. (2015), as implemented in the MWDUST package by Bovy et al. (2016), and combined this with independent random normal samples for the apparent magnitude and $T_{\rm eff}$ to calculate luminosities (Table 2, column 8) and hence radii (Table 2, column 9). Bolometric corrections were derived by linearly interpolating $T_{\rm eff}$, $\log g$, [Fe/H] and $A_{\rm V}$ in the MIST/C3K grid (Conroy et al., in preparation[5]), but $\log g$ had little effect on the result (0.5 dex shifts changed the correction by 0.006 mag). The resulting distributions were used to calculate the mode and 1σ confidence interval for luminosities. We also used the grid-modelling method in ISOCLASSIFY as an alternative approach, which allowed us to fit for reddening. This yielded consistent results to the direct method. Finally, we derived the predicted $\nu_{\rm max}$ values listed in Table 2 (column 10).

4 SEISMIC DATA ANALYSIS

The SONG power spectra of our stars are shown in Fig. 3 (grey curves); all showing clear excess power from oscillations. As expected, the granulation background at low frequencies from velocity measurements is much lower than is typically seen from photometry (Stello et al. 2015, their fig. 2).

Also, because these are short single-site radial-velocity observations, our *Kepler* pipeline (Huber et al. 2009) for measuring $\nu_{\rm max}$ is not suited for these data. Nevertheless, we use the same basic approach as described in Huber et al. (2009) for locating $\nu_{\rm max}$, and an approach similar to that by Mosser & Appourchaux (2009) for measuring and subtracting the noise. The location of $\nu_{\rm max}$ (large black dot) is found as the highest point of the heavily smoothed spectra (black curves) after subtracting the background noise estimated by a linear fit to the noise on either side of the oscillation power. However, we stress that ignoring the slope in noise did not

[3] The accuracy of $\nu_{\rm max}$ also reached about 15 per cent, measured as the average deviation of individual segment $\nu_{\rm max}$ values from the reference value based on the full 30-night data set.

[4] https://github.com/danxhuber/isoclassify
[5] http://waps.cfa.harvard.edu/MIST/model_grids.html

Downloaded from https://academic.oup.com/mnras/article/472/4/4110/4107124 by guest on 23 April 2024

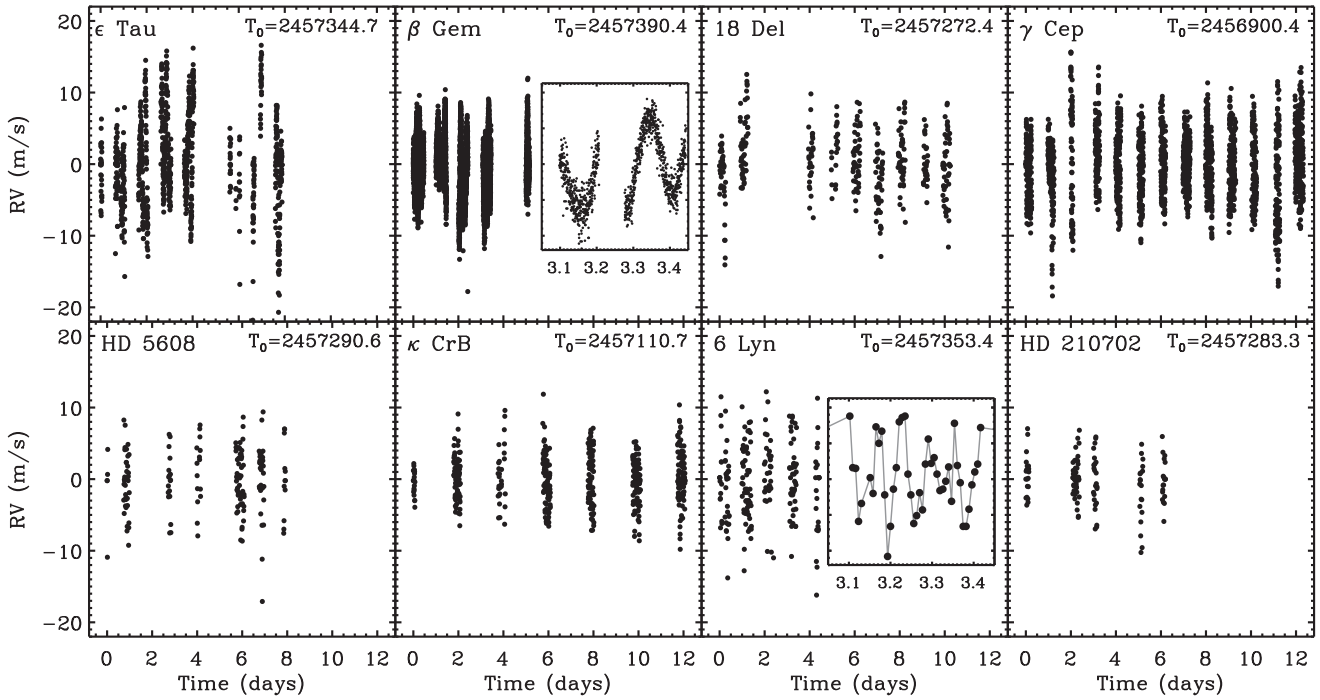

Figure 2. Radial-velocity time series of the eight planet-hosting stars. The time, T_0 (BJD), of the first data point is indicated. For the stars β Gem and 6 Lyn, the inset shows a single night of observation.

Table 2. Observed parameters of the planet-hosting targets.

	Literature						Derived			Asteroseismology		
Star	$\log g$ (dex)[a]	$T_{\rm eff}$ (K)[a]	[Fe/H] (dex)[a]	π (mas)[b]	M ($M_\odot$)[a]	$M_{\rm old}$ ($M_\odot$)[c]	L ($L_\odot$)	R ($R_\odot$)	$\nu_{\rm max,\,pre}$ (μHz)	$\nu_{\rm max,\,obs}$ (μHz)[h]	$\log g$ (dex)	M ($M_\odot$)
(1)	(2)	(3)	(4)	(5)	(6)	(7)	(8)	(9)	(10)	(11)	(12)	(13)
ϵ Tau	2.62(15)	4746(70)	0.17(6)	22.24(25)	2.73(10)	2.70[d]	75.54(1.80)	11.8(5)	64.8(5.4)	56.9(8.5)	2.67(8)	2.40(36)
β Gem	2.91(13)	4935(49)	0.09(4)	96.54(27)	2.08(9)	1.86[d]	36.50(1.69)	8.21(37)	101(10)	84.5(12.7)	2.84(8)	1.73(27)
18 Del	3.08(10)	5076(38)	0.0(?)	13.28(31)	2.33(5)	2.30[e]	33.52(1.77)	7.51(34)	137(12)	112(17)	2.97(9)	1.92(30)
γ Cep	3.10(27)	4764(122)	0.13(6)	70.91(40)	1.26(14)	1.59[d]	11.17(16)	4.88(22)	177(24)	185(28)	3.17(8)	1.32(20)
HD 5608	3.25(16)	4911(51)	0.12(3)	17.74(40)	1.66(8)	1.55[f]	12.74(62)	4.89(23)	228(23)	181(27)	3.17(8)	1.32(21)
κ CrB	3.15(14)	4876(46)	0.13(3)	32.79(21)	1.58(8)	1.80[g]	11.20(17)	4.70(20)	241(21)	213(32)	3.24(8)	1.40(21)
6 Lyn	3.16(5)	4978(18)	−0.13(2)	17.92(47)	1.82(13)	1.82[e]	13.74(73)	5.01(25)	243(28)	183(27)	3.18(9)	1.37(22)
HD 210702	3.36(8)	5000(44)	0.04(3)	18.20(39)	1.71(6)	1.85[d]	12.33(52)	4.68(22)	258(23)	223(33)	3.26(9)	1.47(23)

[a]Source: EOD (exoplanets.org) that refers to Mortier et al. (2013) except for 6 Lyn for which it is Sato et al. (2008) ($\log g$, $T_{\rm eff}$ and [Fe/H]) and Bowler et al. (2010) (M). Although the quoted uncertainties are typically below 50 K ($T_{\rm eff}$) and 0.04 dex ([Fe/H]), we assume $\sigma_{T_{\rm eff}} = 100$ K and $\sigma_{\rm [Fe/H]} = 0.1$ dex to derive columns 8–10 and 12–13.

[b]Source: *Hipparcos* (van Leeuwen 2007). We note that HD 5608 also has a TGAS parallax of 17.13(33)mas (Gaia Collaboration et al. 2016), which would push its inferred (spectroscopic and seismic) masses up by about 0.1 $M_\odot$.

[c]Masses in the EOD before the Mortier et al. (2013) updates, and originally disputed by Lloyd (2011).

[d]Johnson et al. (2007a); HD 5608 and γ Cep were not part of the original disputed set.

[e]Bowler et al. (2010).

[f]Sato et al. (2012).

[g]Johnson et al. (2008).

[h]We adopt an uncertainty of 15 per cent in $\nu_{\rm max,\,obs}$ (Section 4).

Note. Uncertainties are shown in compact bracket form: e.g. 2.35(5) = 2.35 ± 0.05, 2.35(15) = 2.35 ± 0.15, 15.6(1.3) = 15.6 ± 1.3.

change the $\nu_{\rm max}$ estimate significantly (below 1 per cent), suggesting that our adopted method for measuring the noise does not affect our conclusions. The observed $\nu_{\rm max}$ values are listed in Table 2 (column 11). We adopted an uncertainty of 15 per cent on $\nu_{\rm max\,obs}$ according to our derivation from the ξ Hya observations, which was based on the scatter between independent short time series (Section 2). We regard this as a conservative estimate because it accounts for the systematic uncertainty arising from the stochastic nature of the oscillations, which can cause the power excess on a single star basis to be skewed differently from epoch to epoch. This systematic uncertainty is much larger than the statistical uncertainty in measuring $\nu_{\rm max}$ on a single data set when the length of the time series is comparable to, or shorter than, the mode lifetime (as in our case; Dupret et al. 2009; Corsaro, De Ridder & García 2015). In comparison to our adopted conservative uncertainty of 15 per cent, we note that γ Cep has roughly 60 consecutive nights of observation

Downloaded from https://academic.oup.com/mnras/article/472/4/4110/4107124 by guest on 23 April 2024

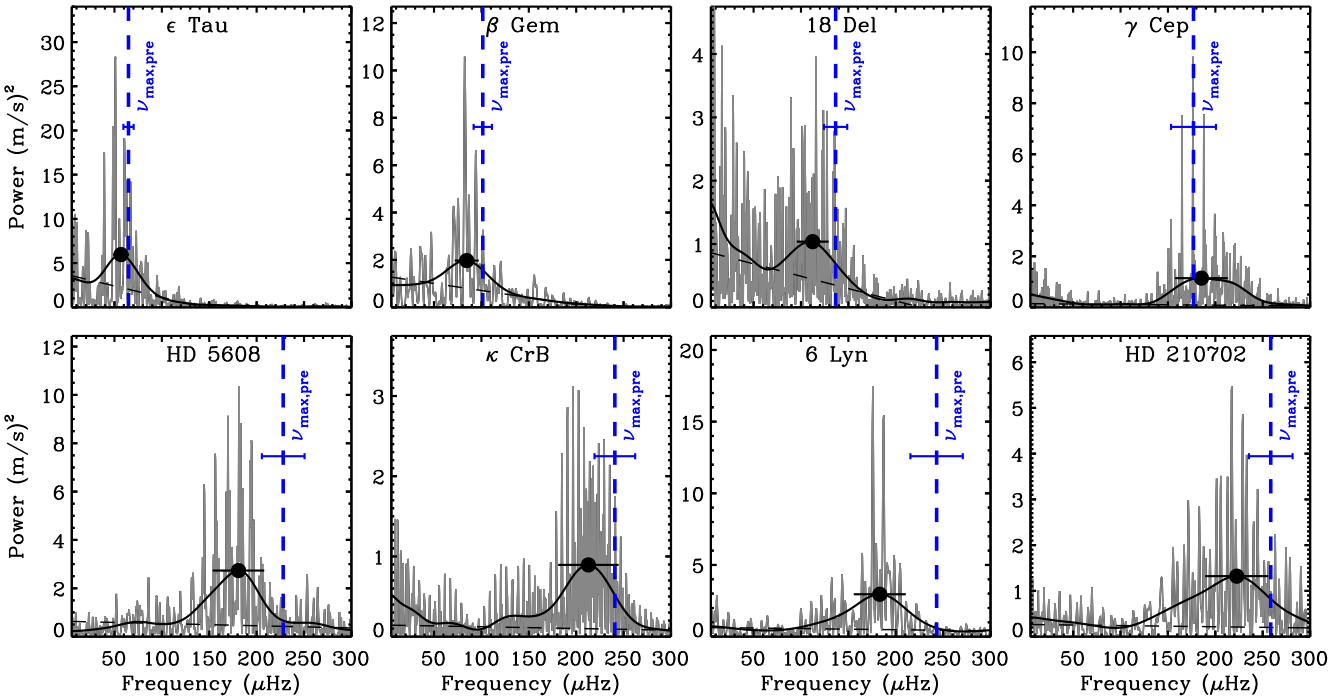

Figure 3. Power spectra of the eight planet-hosting stars (ordered by ν_{max}). The smoothed spectra (black curves) and the location of the observed ν_{max} are shown (large dot), including 1σ error bars. The vertical blue dashed lines indicate the predicted ν_{max} assuming the stellar mass in the EOD. The uncertainty on its location is shown by the blue error bar. The dashed black line shows the noise level in the region around the oscillations.

from another SONG programme (Palle et al., in preparation), which shows only 5 per cent scatter in ν_{max} across 5–10-d segments. From $\nu_{max,\,obs}$ and equation (1), we derived the asteroseismic $\log g$ (column 12), using T_{eff} (column 3) and derived the seismic mass (column 13) using also $L/L_{\odot}$ (column 8). We remind the reader that because our time series are short and single-site observations, we cannot determine individual frequencies or $\Delta\nu$, in order to get additional seismic mass diagnostics.

It is evident from Fig. 3 that all but one star show the oscillation power centred below the predicted ν_{max} shown by the blue vertical dashed lines. Individually, they would all be regarded 'in agreement' with the observations at the 2σ level, but as an ensemble maybe not so. Under the assumption that the predicted ν_{max} values are equal to the true values, the chance of observing a lower ν_{max} in seven out of eight stars is only ∼3 per cent, without taking into account the magnitude of the difference between predicted and observed values. However, a matched *t*-test across the ensemble shows the absolute differences to be highly significant; we can reject the H0 hypothesis (that the predicted and observed values have a common average) at the 0.5 per cent level (1.1 per cent if we had ignored the likely clump stars, Table 1). Hence, this shows a systematic overestimation of the predicted ν_{max}. The ratio between the predicted and observed ν_{max} ranges from 0.95 to 1.33 across the sample, with an average of 1.17 ± 0.04 (the same if we had ignored clump stars). If this difference is entirely due to the adopted stellar mass for predicting ν_{max}, it suggests that the previously published spectroscopic-based masses that we adopted for these stars were generally overestimated by that factor (compare Table 2 columns 6 and 13). Interestingly, the star that agrees best with the seismology (γ Cep) has a dynamic mass of $1.40 \pm 0.12\,M_{\odot}$ (Neuhäuser et al. 2007) and was not included in the retired A-star sample by Johnson et al. (2007a). We note that, on average, the spectroscopic-to-seismic mass ratio would have been 1.24, if we had adopted the masses (Table 2, column 7) and associated spectroscopic T_{eff} and [Fe/H], which were in the EOD at the time they were disputed by Lloyd (2011). It is also noticeable that the scatter between the two sets of spectroscopic masses (Table 2, columns 6 and 7) is larger than suggested by their formal uncertainties. In the following, we look into which factors other than adopted mass could make our predicted ν_{max} consistently too large.

4.1 Potential systematics

If our adopted temperature scale is off, it would affect all parameters that go into predicting ν_{max} (equation 1). Re-running ISOCLASSIFY with a 100 K cooler T_{eff} input results in an estimated luminosity increase of 4 per cent and a mass decrease of 2–3 per cent, in addition to the 7 per cent decrease in $T_{eff}{}^{3.5}$, which all combined decreases the estimated ν_{max} by 14 per cent[6]. Hence, the predicted ν_{max} would agree with the observations if our adopted T_{eff} scale was too hot by 100–150 K. There is indeed large scatter in T_{eff} for these stars in the literature (see SIMBAD), but little empirical evidence to which T_{eff} scale is the most correct one for these stars. The most fundamental test of T_{eff} comes from interferometry. For the three stars in common with our sample, we compared our adopted spectroscopic T_{eff} with the scale found from interferometric angular diameters and bolometric fluxes by White et al. (in preparation). It shows that our adopted T_{eff} is the same for 6 Lyn, 9 K hotter for κ CrB and 50 K hotter for HD 210702, suggesting our T_{eff} scale is not too

[6] Here, we assumed that we could approximate the effect from such a T_{eff} shift on the adopted spectroscopic-based mass by the mass change seen when running ISOCLASSIFY in the grid-based mode with two T_{eff} scales essentially replicating the typical spectroscopic-based approach for estimating stellar mass.

Downloaded from https://academic.oup.com/mnras/article/472/4/4110/4107124 by guest on 23 April 2024

hot at the 100–150 K level, and hence does not support the notion that the discrepancy in Fig. 3 is caused by our $T_{\rm eff}$ scale being too hot. We note that there is some tension between interferometric angular diameters measured from different instruments and thus the adopted $T_{\rm eff}$ scale (e.g. Casagrande et al. 2014; Huber et al. 2017, and references therein), but the higher spatial resolution optical interferometry by White et al. should be less affected by systematic errors than previously published values.

Turning our attention to the adopted metallicities, we see significant scatter across literature values. As noted earlier, we tried to compensate by adopting a larger metallicity uncertainty than quoted in Table 2. However, a systematic shift in metallicity of +0.1 dex would change our predicted $\nu_{\rm max}$ by about 1 per cent for clump stars and 4 per cent for red-giant-branch stars; a change totally dominated by the change in the adopted spectroscopic-based mass. Again, this is assessed using ISOCLASSIFY in its grid-based mode. This mass–metallicity dependence is illustrated by the small black arrow in Fig. 1 (lower right). Although there are no indications of the adopted [Fe/H] being systematically off, such metallicity systematics could only play a minor role in loosening the tension between the predicted and observed $\nu_{\rm max}$.

Finally, could the $\nu_{\rm max}$ scaling relation be systematically off by 15–20 per cent for red giants, resulting in overprediction of $\nu_{\rm max}$? The most direct test of this relation for red giants was carried out by Gaulme et al. (2016). They used oscillating giants in eclipsing binaries to measure a dynamic $\log g$, and hence $\nu_{\rm max}$ given $T_{\rm eff}$, totally independent of seismology. Comparing that with the seismically measured $\nu_{\rm max}$ showed agreement within 3–4 per cent (their fig. 7). We note that their sample comprised generally more evolved stars (lower $\log g$) than ours and the larger $\log g$ stars showed the lowest discrepancies. Huber et al. (2012) used interferometry to obtain independent measurements of stellar radius, which combined with the relation $\Delta\nu \simeq M^{0.5}R^{-1.5}$ (all in solar units) provides mass and hence an expected $\nu_{\rm max}$, given $T_{\rm eff}$. Although the uncertainties on their scaled $\nu_{\rm max}$ values were relatively large, their result (their fig. 8) rules out a systematic error at the 15–20 per cent level required to explain the $\nu_{\rm max}$ difference seen in Fig. 3. Most other studies attempting to verify the seismic-inferred mass from scaling use the relation $M \simeq {\nu_{\rm max}}^3 \Delta\nu^{-4} {T_{\rm eff}}^{1.5}$ (all in solar units), which has a much stronger dependence on $\nu_{\rm max}$ than equation (1), and a high dependence on $\Delta\nu$, and their results are hence not directly applicable to our case. In summary, it seems unlikely that equation (1) is off by 15–20 per cent. However, we note that additional confirmation of the $\nu_{\rm max}$ relation will have to wait till the *Gaia* DR2 results are published, in addition to more interferometric measurements of red giants.

5 CONCLUSION

We used radial-velocity time series from the ground-based SONG telescope to determine the asteroseismic masses of eight planet-hosting red giants ('retired A-stars'). Three are possibly helium-core burning clump stars, while the rest are unambiguously in the ascending red-giant-branch phase. While our observations are too short to firmly establish the mass with high precision for individual stars, our sample is large enough to make conclusions on the ensemble. Based on our reported systematic offset between predicted and observed $\nu_{\rm max}$ of 15–20 per cent, the results indicate that the previous mass determinations adopted here, which were based purely on spectroscopic constraints, are on average overestimated by about 15–20 per cent for these evolved stars, at least those with $M_{\rm spec} \gtrsim 1.6\,{\rm M}_{\odot}$. This conclusion assumes that potential systematics from the adopted $T_{\rm eff}$ scale and the $\nu_{\rm max}$ scaling relation are negligible. Based on our findings, these potential systematics could conspire and add up to a 4–5 per cent contribution of the observed offset. Our result seems consistent with the offset found by Hjørringgaard et al. (2017) for the $M_{\rm spec} \sim 1.9\,{\rm M}_{\odot}$ giant HD 185351, and the lower offset (though within 1σ) found by Campante et al. (2017) for the $M_{\rm spec} \sim 1.5\,{\rm M}_{\odot}$ giant HD 212771 compared to Mortier et al. (2013, our main source of spectroscopic-based results). Our results also seem compatible with North et al. (2017) who find no mass offset on average for their generally lower mass sample of red giants.

From 2018, many of the evolved planet hosts will be observed by *TESS* for at least one month (Ricker et al. 2014). From these data, we can expect to measure $\nu_{\rm max}$, and probably $\Delta\nu$, and for those in the *TESS* continuous viewing zones, we should be able to also measure ΔP of the g modes, which provides additional constraints to the modelling (Hjørringgaard et al. 2017). These investigations will be further enhanced by including *Gaia* DR2 parallax measurements into the mass estimates, reducing observational uncertainties that will enable precise mass estimates on each single star, and not just the ensemble. *Gaia* DR2 will also provide confirmation of the $\nu_{\rm max}$ scaling relation independent of those already at hand from eclipsing binaries and interferometry.

ACKNOWLEDGEMENTS

This research was based on observations made with the Hertzsprung SONG telescope operated on the Spanish Observatorio del Teide on the island of Tenerife by the Aarhus and Copenhagen Universities and by the Instituto de Astrofísica de Canarias. We would like to acknowledge the Villum Foundation, The Danish Council for Independent Research – Natural Science, and the Carlsberg Foundation for their support in building the SONG prototype on Tenerife. Funding for the Stellar Astrophysics Centre is provided by The Danish National Research Foundation (Grant DNRF106). The research was supported by the ASTERISK project (ASTERoseismic Investigations with SONG and *Kepler*) funded by the European Research Council (Grant agreement no.: 267864). DS acknowledges support from the Australian Research Council. PLP acknowledges the support of the Spanish Ministry of Economy and Competitiveness (MINECO) under grant AYA2016-76378-P. LC gratefully acknowledges support from the Australian Research Council (grants DP150100250 and FT160100402). This research has made use of the EOD and the Exoplanet Data Explorer at exoplanets.org. We thank Joel Zinn for helpful discussion.

REFERENCES

Alonso A., Arribas S., Martínez-Roger C., 1999, A&AS, 140, 261
Andersen M. F. et al., 2014, Rev. Mex. Astron. Astrofis., 45, 83
Antoci V. et al., 2013, MNRAS, 435, 1563
Beck P. G. et al., 2012, Nature, 481, 55
Bedding T. R. et al., 2011, Nature, 471, 608
Bovy J., Rix H.-W., Green G. M., Schlafly E. F., Finkbeiner D. P., 2016, ApJ, 818, 130
Bowler B. P. et al., 2010, ApJ, 709, 396
Brown T. M., Gilliland R. L., Noyes R. W., Ramsey L. W., 1991, ApJ, 368, 599
Butler R. P., Marcy G. W., Williams E., McCarthy C., Dosanjh P., Vogt S. S., 1996, PASP, 108, 500
Campante T. L. et al., 2017, MNRAS, 469, 1360
Casagrande L. et al., 2014, MNRAS, 439, 2060
Corsaro E., De R. J., García R. A., 2015, A&A, 579, A83

Downloaded from https://academic.oup.com/mnras/article/472/4/4110/4107124 by guest on 23 April 2024

Dupret M. et al., 2009, A&A, 506, 57
Frandsen S. et al., 2002, A&A, 394, L5
Gaia Collaboration et al., 2016, A&A, 595, A1
Gaulme P. et al., 2016, ApJ, 832, 121
Green G. M. et al., 2015, ApJ, 810, 25
Grundahl F. et al., 2017, ApJ, 836, 142
Hjørringgaard J. G., Silva A. V., White T. R., Huber D., Pope B. J. S., Casagrande L., Justesen A. B., Christensen-Dalsgaard J., 2017, MNRAS, 464, 3713
Huber D., Stello D., Bedding T. R., Chaplin W. J., Arentoft T., Quirion P., Kjeldsen H., 2009, Commun. Asteroseismol., 160, 74
Huber D. et al., 2012, ApJ, 760, 32
Huber D. et al., 2017, ApJ, 844, 102
Høg E. et al., 2000, A&A, 355, L27
Jofré E., Petrucci R., Saffe C., Saker L., de la Villarmois E. A., Chavero C., Gómez M., Mauas P. J. D., 2015, A&A, 574, A50
Johnson J. A., Marcy G. W., Fischer D. A., Henry G. W., Wright J. T., Isaacson H., McCarthy C., 2006, ApJ, 652, 1724
Johnson J. A. et al., 2007a, ApJ, 665, 785
Johnson J. A., Butler R. P., Marcy G. W., Fischer D. A., Vogt S. S., Wright J. T., Peek K. M. G., 2007b, ApJ, 670, 833
Johnson J. A., Marcy G. W., Fischer D. A., Wright J. T., Reffert S., Kregenow J. M., Williams P. K. G., Peek K. M. G., 2008, ApJ, 675, 784
Johnson J. A., Aller K. M., Howard A. W., Crepp J. R., 2010, PASP, 122, 905
Johnson J. A., Morton T. D., Wright J. T., 2013, ApJ, 763, 53
Johnson J. A. et al., 2014, ApJ, 794, 15
Kallinger T. et al., 2010, A&A, 509, 77
Kjeldsen H., Bedding T. R., 1995, A&A, 293, 87
Lloyd J. P., 2011, ApJ, 739, L49
Lloyd J. P., 2013, ApJ, 774, L2
Mortier A., Santos N. C., Sousa S. G., Adibekyan V. Z., Delgado M. E., Tsantaki M., Israelian G., Mayor M., 2013, A&A, 557, A70
Mosser B., Appourchaux T., 2009, A&A, 508, 877
Mosser B. et al., 2012, A&A, 548, A10
Neuhäuser R., Mugrauer M., Fukagawa M., Torres G., Schmidt T., 2007, A&A, 462, 777
North T. S. H. et al., 2017, MNRAS, preprint (arXiv:1708.00716)
Paxton B. et al., 2013, ApJS, 208, 4
Piskunov N. E., Valenti J. A., 2002, A&A, 385, 1095
Ricker G. R. et al., 2014, in Oschmann J. M., Jr, Clampin M., Fazio G. G., MacEwen H. A., eds, Proc. SPIE Conf. Ser. Vol. 9143, Space Telescopes and Instrumentation 2014: Optical, Infrared, and Millimeter Wave. SPIE, Bellingham, p. 914320
Ritter A., Hyde E. A., Parker Q. A., 2014, PASP, 126, 170
Sato B. et al., 2008, PASJ, 60, 1317
Sato B. et al., 2012, PASJ, 64, 135
Schlaufman K. C., Winn J. N., 2013, ApJ, 772, 143
Stello D., Kjeldsen H., Bedding T. R., De Ridder J., Aerts C., Carrier F., Frandsen S., 2004, Sol. Phys., 220, 207
Stello D., Bruntt H., Preston H., Buzasi D., 2008, ApJ, 674, L53
Stello D. et al., 2013, ApJ, 765, L41
Stello D. et al., 2015, ApJ, 809, L3
Stello D., Cantiello M., Fuller J., Huber D., García R. A., Bedding T. R., Bildsten L., Silva Aguirre V., 2016, Nature, 529, 364
van Leeuwen F., 2007, Astrophysics and Space Science Library, Vol. 350, Hipparcos, the New Reduction of the Raw Data. Springer, Berlin
Wright J. T. et al., 2011, PASP, 123, 412

This paper has been typeset from a TEX/LATEX file prepared by the author.

Downloaded from https://academic.oup.com/mnras/article/472/4/4110/4107124 by guest on 23 April 2024